A HYDRODYNAMIC MODEL OF WIRE DRAWING

A Thesis Submitted
in Partial Fulfilment of the Requirements
for the Degree of
MASTER OF TECHNOLOGY

By
DRUPAD RAM

to the
DEPARTMENT OF MECHANICAL ENGINEERING
INDIAN INSTITUTE OF TECHNOLOGY, KANPUR
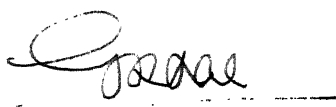AUGUST, 1978

ME-1978-M-RAM-HYD

DEDICATED TO

MY BELOVED FATHER
WHOM I LOST FOR EVER
DURING MY M.TECH. PROGRAMME

AND ALSO

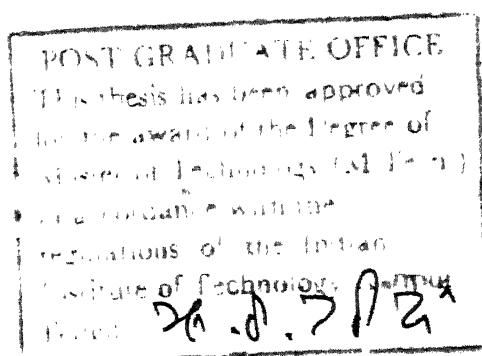TO MY MOTHER, BROTHERS, SISTERS
AND WIFE

CERTIFICATE

Certified that the work entitled, 'A Hydrodynamic Model of Wire Drawing', which is being submitted by Mr. Drupad Ram in partial fulfilment of the award of the degree of Master of Technology, has been carried out under my supervision and has not been submitted elsewhere for the award of a degree.

Dr. G.K. Lal
Professor
Department of Mechanical Engg.
Indian Institute of Technology
August, 1978   Kanpur 208016

ACKNOWLEDGEMENTS

It gives me a great pleasure to express my heart-felt gratitude towards Dr. G.K. Lal for his constant encouragement timely guidance, invaluable comments and fruitful criticism throughout the course of this work.

I acknowledge with thanks the invaluable cooperation and timely help received from Messrs. Ram Jiyawan, S.K.Urmal H.K. Dey Sarkar and T. Ram. I owe my thanks to all my friends who helped me one way or the other through out this work.

I am thankful to Mr. D.K. Misra for his timely help in tracing the figures. Thanks are also due to Mr.J.K.Mi for his patient and accurate typing.

I must express my appreciation to Messrs. D.P. Saini Ayodhya Prasad and Lalta Prasad for their useful cooperatio during the programme.

I must express my deep sense of gratitude to thousands of people whose love and affection has always given me encouragement to come over the difficulties in my life.

August, 1978.   Drupad Ram

CONTENTS

          LIST OF FIGURES   v

          NOMENCLATURE   vi

          SYNOPSIS   ix

  I.   INTRODUCTION

          1.1   Introduction   1

          1.2   Lubrication and Friction in Wire
                Drawing   1

          1.3   Deformation of Wire Material   4

          1.4   Hydrodynamic Models   6

          1.5   Present Work   7

  II.   THEORETICAL ANALYSIS

          2.1   Introduction   9

          2.2   Basic Assumptions   9

          2.3   Additional Assumptions   10

          2.4   Application of the Minimum Energy
                Production Rate Principle   11

          2.5   Analysis   12

          2.5.1 Principle of Minimum Energy Production
                Rate   14

          2.5.2 Strain-Hardening Effect   20

          2.5.3 Redundant Work   21

          2.5.4 Strain-rate and Temperature Effects   22

  III. RESULTS AND DISCUSSION   28

  IV.   CONCLUSION   34

          REFERENCES   35

          APPENDIX 1

LIST OF FIGURES

NOMENCLATURE

A	$=$	Area of cross-section of the wire
A'	$=$	Material constant in equation (37b)
B	$=$	Material constant in equation (37a)
B'	$=$	Material constant in equation (37b)
C	$=$	Constant, defined by equation (25)
C_1	$=$	Constant, defined by equation (27)
D	$=$	Diameter of wire
$\bar{D}$	$=$	D/D_2 .
$\bar{e}$	$=$	Generalised plastic strain
e_x	$=$	Strain at cross-section X
$F(\alpha)$	$=$	Defined in equation (52)
f	$=$	Redundant work factor
$g(z)$	$=$	Defined in equation (42)
H	$=$	Lubricant film thickness
H_2	$=$	Minimum film thickness
$\bar{H}$	$=$	H/H_2, Dimension-less film thickness
ΔH	$=$	Activation energy
K	$=$	Yield-stress of the material (Equation (44))
L	$=$	Spherical surface as shown in Fig. 2.2.
m	$=$	Material constant in equation (37a)
m'	$=$	Material constant in equation (37b)
n	$=$	Material constant defined in equation (43)
p	$=$	Normal pressure of lubricant
Q	$=$	Volume flow-rate of lubricant

R	$=$	Fractional Reduction in area of wire $= (A_1-A_2)/A_1$
R'	$=$	Gas constant
R_1, R_2	$=$	Entry and exit radius of wire, respectively
$r, \theta, \emptyset$	$=$	Spherical coordinate system
s	$=$	Coordinate measured along die-taper
T	$=$	Temperature of operation in $^\circ K$
T_1	$=$	$t_1/\bar{\sigma}_0$,
T_2	$=$	$t_2/\bar{\sigma}_0$
T_{11}, T_{22}	$=$	Temperatures
T_H	$=$	Homologous temperature
t_1, t_2	$=$	Tensile stresses at ends
u	$=$	velocity of lubricant along the wire surface
V	$=$	Axial velocity of the wire
$\bar{V}$	$=$	Average velocity of lubricant
v	$=$	Volume of deformation zone II
$\dot{v}$	$=$	Volume flow-rate of deformed material.
W_1	$=$	Defined in equation (30a)
W_2	$=$	Defined in equation (30b)
$\dot{W}_p$	$=$	Rate of plastic work
$\dot{W}_s$	$=$	Rate of shear work
X	$=$	Distance measured along the axis of the wire
z	$=$	Zener-Hollomon parameter defined in equation (42)

Greek Symbols;

α	=	Semi-die angle
η	=	Dynamic viscosity of lubricant
γ	=	Coefficient of viscosity
σ	=	Direct stress
σ_e	=	Stress at a given strain e
$\bar{\sigma}$	=	Generalised plastic stress
$\bar{\sigma}_0$	=	Generalised yield-stress of material before drawing
σ_x	=	Tensile stress at cross section X
σ'_x	=	$\sigma_x/\bar{\sigma}_0$
τ	=	Shear stress
μ_a	=	Apparent coefficient of friction
μ_0	=	Defined in equation (35)
ε_0	=	$2 \ln (R_1/R_2)$
$\dot{\varepsilon}$	=	Strain-rate
$\bar{\dot{\varepsilon}}$	=	Effective average strain-rate

Subscripts:

1	=	Entry point
2	=	Exit point

SYNOPSIS

Several attempts have been made in the past to analyse the wire drawing operation but most of these theories have been worked out for dry friction conditions assuming constant and uniform coefficient of friction throughout the die-work interface. In the present work, an attempt has been made to propose a hydrodynamic model of wire drawing incorporating the effects of lubrication, friction, strain, strain-rate, temperature and redundant work. The principle of minimum energy production rate has been used to evaluate minimum film thickness.

The theoretical results indicate that the apparent coefficient of friction increases with increase in semi-die-angle but decreases with increase in reduction. Results show that there exists an optimum die-angle which gives the minimum drawing stress. This optimum die-angle, however, depends on reduction. The optimum die-angle appears to increase linearly with increase in reduction, in the practical range of reduction, when strain, strain-rate and temperature effects are incorporated.

Comparison with published experimental results shows reasonably close agreement.

CHAPTER I

INTRODUCTION

1.1 Introduction:

In wire drawing operation, the wire is generally
pulled through a number of dies. While passing through the
die (Fig. 1.1), the wire deforms plastically in the contact
zone and reduction in diameter is achieved. The cylindrical
portion of die, called the bearing zone, is provided for the
dimensional stability of the product,although it results in
additional frictional loss. To reduce the frictional
losses and increase the life of die, lubricants are used.
Phenomenons occurring inside the deformation zone are very
complex and are still not clearly understood.

1.2 Lubrication and Friction in Wire Drawing:

As the wire passes through the die, there is relative
motion between the wire and die surface which causes sliding
friction. The primary mechanism of friction is recognised as
the formation and rupture of minute bridges between asperties
of sliding surfaces. The function of a lubricant is to separate
the sliding surfaces by a thin film, thus reducing the metal to
metal contact, the film itself being easily sheared. This
phenomenon, according to the film thickness could be classified
into two extreme types: boundary and hydrodynamic lubrication.

Boundary layer lubrication is said to prevail when the film thickness is only one or two molecular layer thick and it takes place under high normal pressures and low sliding speeds [1]. Friction is influenced by the nature of the underlying metal surface and chemical nature of the lubricant, but not by the bulk properties of the lubricant such as density and viscosity.

In hydrodynamic lubrication, the lubricant film is of appreciable thickness such that it completely separates the sliding surfaces and resistance to sliding motion is entirely due to viscosity and other bulk properties of the lubricant. It takes place when the pressure developed between the die and wire due to the lubricant film is sufficient to keep the sliding surfaces apart. The required condition for building up such an oil wedge prevails at high speeds. The typical friction-velocity curve [1], at a given pressure, for a pair of sliding surfaces capable of hydrodynamic lubrication, is shown in Fig. 1.2. After a critical velocity, hydrodynamic lubrication takes place. Besides this, it also depends on the pressure, viscosity, surface roughness and sliding geometry. When wire is passed through pressurised chamber, the hydrodynamic effect does not depend entirely on the speed, viscosity, or chamber or tube length [2]. In this case, the flow of lubricant at sufficient pressure ensures the existence of hydrodynamic boundary layer lubrication.

Experimental observations [3] have established the
fact that the amount of the lubricant which passes through
the die is often much greater than that corresponding to a
molecular thickness of the kind which covers the surface under
boundary layer lubrication conditions. Moreover, there
exists appreciable electrical resistance between wire and
die and it increases with increase in the drawing speed.
Christopherson and Naylor [3] estimated the oil film thick-
ness to be of the order of 10^{-4} cm. Wistreich [4] has also
discussed the existence of full fluid film lubrication. These
experiments lead to the conclusion that hydrodynamic lubrica-
tion condition exists after a critical speed.

For a given set of wire drawing conditions, the drawing
stresses etc. can be calculated by assuming a constant and
uniform coefficient of sliding friction between the wire and
die surfaces. Results obtained, however, show significant
deviation in the coefficient of sliding friction [5]. Therefore,
the coefficient of friction must be derived either from test
results or through analytical methods. Wistreich [6], Yang [7]
have estimated the coefficient of friction under dry
friction conditions. Under hydrodynamic lubrication, the
coefficient of friction varies significantly with speed,
viscosity, die-angle , reduction and other bulk properties
of the lubricant [2].Due to frictional losses, there is rise
in the bulk temperature which can affect the bulk properties

of the lubricant. At speeds below the critical speed where
hydrodynamic lubrication is not achieved, the roughness or
the asperties are the main cause of friction.

Crook [8] has shown that for sliding speeds of
70-500 in/sec. the thickness of the lubricant film formed
between elastic discs rotating about parallel axes and
subjected to pressure varied from 1×10^{-4} to 2×10^{-4} cm,
when the discs surfaces are ground and lapped. He further
reported that full fluid film was established due to the
tendency of the fluid viscosity to rise rapidly with increas-
ing pressure. Shaw and Mack [9] have showed that the visco-
sity of the mineral oil may be increased by a factor of
over 100 when the pressure is raised from 1 to 4000 atmosphere.
They further reported the exponential fall in viscosity
with rise in temperature. This effect may be dependent on
the residence time also. In case of wire drawing, the visco-
sity at average pressure can be taken to avoid any further
complexity in the calculation.

1.3 Deformation of Wire Material:

With increasing drawing speed the rate of straining
of the wire material will increase. Also the level of flow
stress curve tends to increase with increasing rate of
strain [10]. The stress-strain curve of the metal is also
sensitive to temperature, the yield stress falling with
increasing temperature [10].

Wistreich [6] has reported an extensive experimental
study to determine the effects of reduction and cone angle
on the drawing stress. After drawing the wire through
succession of dies and testing the wire specimens at
various stages, significant strain hardening effect was
observed. The operation takes place at very high speeds and
therefore, high strain rates are involved in the process.
When a material is deformed at a temperature below its **rs**
recrystallization temperature, it does strain-harden [10].
Alder and Phillips [11] have reported the strain-hardening
effects for various materials and calculated the strain-rate
sensitivity coefficients for a range of temperature ˜ and
reduction assuming that the Ludwik's power law [12] holds.
The stress-strain curve for copper at $750^{\circ}C$ at strain rate
of 12.9 sec^{-1} showed a drop in yield stress above 40 percent
reduction, indicating that softening and strain-hardening
were in balance in this range [11]. In case of aluminium,
the stress-strain curve showed a marked strain-rate effect
at room temperature and continuous rise at all temperature.

Due to frictional heating in the deformation zone and
irreversible plastic deformation of the wire material within
the deformation zone, the temperature of the material rises.
Some of the heat generated will be carried away by the lubri-
cant. Further, if the residence time of the metal in the zone
of deformation is sufficiently short (of the order of few

microseconds), the effect of transient temperature rise during deformation may be insignificant and the thermal softening effect within the deformation zone will probably be small as compared to strain-rate effects [13].

Wistreich [6] reported in his work on wire drawing that the wire radius contracted at the exit to a size smaller than the die radius. If hydrodynamic lubrication prevailed, then this size difference is the lubricant gap. Tattersall [23] points out the possibility of forcing a lubricant film to enter the interface and completely separate the deforming material from the die in the wire drawing.

Due to various combinations of the factors (reduction, die angle, friction, properties of material etc.) affecting the drawing of the wire, lot of manufacturing defects surface out. Snake skin formation, chevroning, dead zone formation, bulging and contraction, shaving etc. are the consequences of such combination of variables. Because of the undesirable combinations of variables, there is considerable gap between the practical results and the theoretical results.

1.4 Hydrodynamic Models:

Hillier [14] assumed the film thickness under hydrodynamic lubrication conditions in the bearing zone and projected this thickness of the film of the lubricant in the deformation zone. Through volume constancy of the

flowing lubricant, he estimated the thickness of the film
in the deformation zone. After calculating all the energy
losses and applying the principle of minimum energy, he
calculated the assumed thickness of the film. In this analysis,
he accounted for the bearing zone losses also.

Bedi [15] assumed the exponential variation of the
film thickness with change in diameter as exponent in the
deformation zone. He calculated the two constants using volume
constancy and the principle of minimum energy production rate
as the conditions. Only the deformation zone was considered
in his analysis and the results were projected for constant film
thickness of the lubricant. In calculating the work done
during plastic deformation of the wire, he accounted only for
the redundant work and strain-hardening and not for the strain-
rate hardening and temperature effect.

1.5 Present Work:

Most of the previous attempts to analyse the wire-
drawing operation have been carried out for dry conditions.
Further, the coefficient of friction along the die and work
surface has been assumed to be constant and uniform throughout
the interface. A few investigators have tried to incorporate
the effects of lubricant. Most notable of these attempts has
been due to Bedi [15]. In the present work, an attempt has
been made to present an analysis of wire drawing operation

considering the effects of lubrication, friction, strain-hardening, strain-rate, temperature and redundant work. The basic formulation, proposed by Bedi [15] has been adopted with certain modifications. Theoretical results have been obtained to study the variation of coefficient of friction, film thickness, drawing stress, optimum die angle etc. with drawing speed, die-angle and reduction.

CHAPTER II

THEORETICAL ANALYSIS

2.1 Introduction:

As discussed earlier, there are various parameters
that significantly affect the wire drawing operation. In a
typical wire drawing operation considered here, a wire of
diameter D_1 is pulled through a conical die and is reduced
to diameter D_2 (Fig. 2.1). In the presence of hydrodynamic
lubrication, the die-work interface is separated by a
lubricant film of thickness H. Depending upon the input
conditions (die-angle, reduction, drawing speed etc.) the
output values such as drawing stress, separating force, etc.
could be evaluated. In order to simplify the analysis
several simplifying assumptions have been made.

2.2 Basic Assumptions:

(a) For Wire Material:

      (1) The material is homogeneous, isotropic and
           plastically incompressible.

      (2) Elastic strains in the material are negligibly
           small as compared to plastic strains.

(3) The flow of the material takes place under isothermal conditions through out the plastic deformation zone, i.e., there is no temperature gradient in the plastic zone.

(4) Yield and flow are independent of the hydrostatic component of the stress.

(5) The material obeys the von-Mises yield criterion and its associated flow rule.

(b) For Lubricant:

(1) Fluid is incompressible and Newtonian.

(2) The flow is laminar and viscous.

(3) Inertia effects are negligible as compared to other forces.

(4) The flow occurs under isothermal conditions.

(5) There is no change in the physical properties of the lubricant due to rise in temperature of the deformation zone.

(6) The lubricant viscosity is independent of the variation in pressure along the die-wire interface.

2.3 Additional Assumptions:

(i) During deformation of the wire, a plane section of the wire remains plane and the deformation of a plane element is homogeneous.

(ii)   Yield is independent of surface shear stresses.

(iii)   There exists complete hydrodynamic lubrication between wire and die and the film extends over the entire interface.

(iv)   The inner surface of the die and outer surface of the wire are comparatively smooth.

(v)   The thickness of the oil film is small in comparison to the diameter of the wire.

2.4 Application of the Minimum Energy Production Rate Principle:

The assumptions made are essentially the same as mentioned above, together with additional simplifying assumptions as follows:

(i)   The lubricant viscosity in the wire and die gap is independent of the variation in the pressure along the die surface.

(ii)   The effect of pressure gradient along the inner face of the die has negligible effect on the surface shear stress.

(iii)   Coefficient of friction is dependent on the oil pressure.

(iv)   Coefficient of viscosity of the lubricant does not change significantly during drawing.

Bedi [15] obtained the film thickness by invoking the principle of minimum energy production rate. As the thickness of the film increases the rate of shear work, $\dot{W}_s$, of the lubricant tends to decrease, but at the same time the

size of the outgoing wire decreases thereby increasing the
rate of plastic work, $\dot{W}_p$. This implies that there has to
be a minimum thickness of the oil film at which the rate of
total energy dissipation will be minimum. This can be calcu-
lated by differentiating the total energy dissipation with
respect to the thickness of the film, H_2, i.e.,

$$\frac{\partial}{\partial H_2} (\dot{W}_p + \dot{W}_s) = 0$$

2.5 Analysis:

Neglecting the redundant work for the time being, the
tensile stress σ_x at section X as shown in Fig. 2.1 is well
known under the above mentioned assumptions and is given by [16],

$$\frac{d\sigma_x}{d\bar{e}} + (\frac{\tau}{p} \cot \alpha) \sigma_x = (1 + \frac{\tau}{p} \cot \alpha) \bar{\sigma} , \qquad (1)$$

where α is the semi-die angle, $\bar{e}$ is the generalised strain,
τ is the shear stress; p is the pressure of the lubricant
and $\bar{\sigma}$ is the generalised yield stress.

In this case,

$$\bar{e} = e_x = \ln (\frac{A_1}{A}) , \qquad (2)$$

where e_x is the strain at cross-section X ; A_1 is the cross-
sectional area of the entering wire and A is the cross-
sectional area of the wire at cross-section X .

The end conditions for equation (1) are:

At entry:

$$\sigma_x = t_1 ; \quad \bar{e}_1 = 0 ,$$

At exit:

$$\sigma_x = t_2; \quad \bar{e} = \bar{e}_2 = \ln \left(\frac{1}{1-R}\right). \tag{3}$$

Here t_1 and t_2 are the back and front drawing stresses, respectively, $\bar{e}_2$ is the generalised strain at the exit and R is the reduction.

For a fully developed Newtonian laminar flow of the lubricant between the die and work, and assuming the taper of the lubricant wedge to be shallow, the generalised Reynold's equation [17] is,

$$\frac{1}{2} Hu - \frac{H^3}{12\eta} \frac{dp}{ds} = Q , \tag{4a}$$

where Q is the volume flow rate of the lubricant,

    u is the velocity of the lubricant along tapered surface,

    H is the film thickness,

    η is the viscosity of the lubricant and

    s is the distance from entry, along the tapered surface.

For incompressible fluid,

$$\frac{\partial Q}{\partial s} = 0. \tag{4b}$$

Pinkus and Sternlicht [17] have showed that the surface shear stress on the wire material due to viscous shearing of the lubricant can be evaluated from,

$$\tau = \eta \frac{u}{H} + \frac{1}{2} H \frac{dp}{ds} . \tag{5}$$

For very small values of H, this expression can be further simplified as,

$$\tau = \eta \frac{u}{H} = \frac{\eta V}{H \cos \alpha} , \tag{6}$$

since $u = \frac{V}{\cos \alpha}$, $\tag{7}$

where, V is the drawing speed.

Also the condition of incompressibility of the material gives,

$$A_1 V_1 = AV = A_2 V_2 ,$$

$$\text{or} \quad D_1^2 V_1 = D^2 V = D_2^2 V_2 , \tag{8}$$

where subscripts 1 and 2 indicate the value of parameters at entry and exit, respectively.

2.5.1 Principle of Minimum Energy Production Rate:

As pointed out earlier, under the conditions assumed, the principle of minimum energy production rate can be expressed as,

$$\frac{\partial}{\partial H_2} (\dot{W}_p + \dot{W}_s) = 0 . \tag{9}$$

For homogeneous deformation, the rate of plastic work is

$$\dot{W}_p = \frac{\pi}{4} D_2^2 V_2 \int_0^{\bar{c}_2} \bar{\sigma} \, d\bar{c} \ . \tag{10}$$

For incorporating the effect of redundant work, $\bar{c}$ is replaced by $\bar{c}^* = f\bar{c}$, where f is known as the redundant work factor. Rowe [18] worked out the value of this factor for a range of metals and lubricants, based on the work of Johnson [12]. Rowe [18] has suggested that this redundant work factor can be expressed in terms of reduction as,

$$f = 0.87 + (\frac{1-R}{R}) \sin \alpha \ . \tag{11}$$

Therefore, after including the redundant work, equation (10) reduces to,

$$\dot{W}_p = \frac{\pi}{4} D_2^2 V_2 \int_0^{\bar{c}_2^*} \bar{\sigma} \, d\bar{c} \ , \tag{12}$$

where,

$$\bar{c}_2^* = f\bar{c}_2 = f \ln(\frac{A_1}{A_2}) = -2 f \ln (\frac{D_2}{D_1}). \tag{13}$$

Therefore,

$$\frac{\partial \dot{W}_p}{\partial H_2} = \frac{\pi}{4} D_2^2 V_2 \left[\frac{\partial}{\partial \bar{c}_2^*} \int_0^{\bar{c}^*} \bar{\sigma} \, d\bar{c} \right] \frac{d\bar{c}_2^*}{dH_2}$$

$$= \frac{\pi}{4} D_2^2 V_2 \bar{\sigma}_2 \frac{d\bar{c}_2^*}{dH_2} \ . \tag{14}$$

where $\bar{\sigma}_2$ is the generalised yield stress at exit.
Now,

$$\frac{d\bar{c}_2^*}{dH_2} = \frac{d\bar{c}_2^*}{dD_2} \cdot \frac{dD_2}{dH_2} = -2 \frac{d\bar{c}_2^*}{dD_2} \ , \tag{15}$$

and equation (13) gives,

$$\frac{d\bar{\sigma}_2^*}{dD_2} = -\frac{2f}{D_2} . \tag{16}$$

Using equations (15) and (16), equation (14) reduces to,

$$\frac{\partial \dot{W}_p}{\partial H_2} = \pi D_2 \, V_2 \, f \, \bar{\sigma}_2 . \tag{17}$$

The total rate of shear work, $\dot{W}_s$, for the lubricant can be evaluated from,

$$\dot{W}_s = \int_S \pi D \, \tau \, u \, ds . \tag{18}$$

Using Fig. (2.1), ds can be evaluated and is given by,

$$ds = -(\tfrac{1}{2} \, \text{Cosec} \, \alpha \, dD + \text{Cot} \, \alpha \, dH) . \tag{19}$$

Therefore, from Equations (7), (18) and (19),

$$\dot{W}_s = -\int_{D_1}^{D_2} \frac{\pi D \, \eta \, V^2}{H \, \text{Cos}^2 \, \alpha} \left[\tfrac{1}{2} \, \text{Cosec} \, \alpha + \text{Cot} \, \alpha \, \frac{dH}{dD} \right] dD . \tag{20}$$

Bedi [15] had assumed exponential variation of the film thickness with exponent as a constant multiplied by the difference in the diameter. Here, however, a linear variation of the film thickness will be assumed for **simplifying the** analysis. Thus the film thickness can be evaluated from,

$$H = H_2 \, [1 + C \, (D - D_2)] , \tag{21}$$

where C is a constant and

H_2 is the thickness of the film at the exit of the die.

Also at the entrance,

$$D = D_1 \text{ and } H = H_1.$$

Therefore:

$$\frac{H_1}{H_2} = 1 + C (D_1 - D_2). \tag{22}$$

For very small film thickness (H) and large peripheral velocity (u) in equation (4a) the flow rate can be approximated by,

$$Q \simeq \tfrac{1}{2} Hu,$$

or

$$H_1 \bar{V}_1 = H_2 \bar{V}_2 = H\bar{V} = Q, \tag{23}$$

where $\bar{V}$ is the average velocity of the lubricant at any section. Therefore, from equations (7), (8) and (23),

$$\frac{H_1}{H_2} = \left(\frac{1}{1-R}\right). \tag{24}$$

Now equations (22) and (24) give,

$$C = \left(\frac{R}{1-R}\right) \cdot \frac{1}{D_2 \left(\sqrt{\frac{1}{1-R}} - 1\right)} \tag{25}$$

Also, from equations (21) and (25),

$$H = H_2 \left[1 + \frac{R}{1-R} \cdot \frac{1}{\sqrt{\frac{1}{1-R}} - 1} (\bar{D} - 1) \right],$$

or

$$H = H_2 \left[1 + C_1 (\bar{D} - 1) \right], \tag{26}$$

where,

$$C_1 = \frac{R}{1-R} \cdot \frac{1}{\left(\sqrt{\frac{1}{1-R}} - 1\right)} , \tag{27}$$

and

$$\bar{D} = D/D_2 .$$

Therefore, from equation (26),

$$\frac{1}{H} \frac{dH}{d\bar{D}} = \frac{C_1/D_2}{1 + C_1(\bar{D}-1)} . \tag{28}$$

Substituting equations (26) and (28) in equation (20), the rate of shear work is,

$$\dot{W}_s = -\int_{D_1}^{D_2} \frac{\pi D V^2 \eta}{\cos^2 \alpha} \cdot \left[\frac{1}{2 H \sin \alpha} + \frac{\cos \alpha}{\sin \alpha} \cdot \frac{1}{H} \frac{dH}{d\bar{D}} \right] dD,$$

or

$$\dot{W}_s = \frac{\pi \eta V_2^2 D_2^2}{2 \cos^2 \alpha \sin \alpha} \left[\frac{W_1}{H_2} + W_2 \right], \tag{29}$$

where,

$$W_1 = \int_1^{\sqrt{1/(1-R)}} \frac{\bar{D}}{1 + C_1(\bar{D}-1)} \, d\bar{D},$$

which can be rewritten as,

$$W_1 = \frac{1}{C_1} \left[\sqrt{\frac{1}{1-R}} - 1 \right] - \frac{1}{C_1^2} \ln \left[1 + C_1 \left(\sqrt{\frac{1}{1-R}} - 1 \right) \right] \tag{30}$$

and,

$$W_2 = \int_1^{\sqrt{1/(1-R)}} \frac{\bar{D}}{1 + C_1(\bar{D}-1)} \cdot \frac{2 \cos \alpha \, C_1}{D_2} \, d\bar{D},$$

or,

$$W_2 = \frac{2V_1}{D_2} C_1 \, \text{Cos} \, \alpha \tag{31}$$

Now, from equation (29),

$$\frac{\partial \dot{W}_s}{\partial H_2} = -\frac{\pi}{2} \cdot \frac{\eta \, V_2^2 \, D_2^2}{\text{Cos}^2 \, \alpha \, \text{Sin} \, \alpha} \cdot \frac{W_1}{H_2^2} \cdot \tag{32}$$

Equations (9), (17) and (32) give,

$$\frac{\partial \dot{W}_p}{\partial H_2} + \frac{\partial \dot{W}_s}{\partial H_2} = 0,$$

or,

$$\pi \, D_2 \, V_2 \, f \, \bar{\sigma}_2 - \frac{\pi}{2} \cdot \frac{\eta \, V_2^2 \, D_2^2}{\text{Cos}^2 \, \alpha . \text{Sin} \, \alpha} \cdot \frac{W_1}{H_2^2} = 0,$$

or

$$\left(\frac{H_2}{D_2}\right)^2 = \frac{1}{2} \left(\frac{\eta \, V_2}{D_2 \, \bar{\sigma}_2}\right) \cdot \left(\frac{W_1}{f \, \text{Sin} \, \alpha \, \text{Cos}^2 \, \alpha}\right) . \tag{33}$$

Therefore, an apparent coefficient of friction, μ_a, can be defined by making use of equations (6), (26) and (33) as follows:

$$\mu_a = \frac{\tau}{p},$$

or

$$\mu_a = \frac{\mu_o}{\sqrt{2}} \sqrt{\frac{f \, \text{Sin} \, \alpha}{W_1}} \left[\frac{1}{1 + C_1 \, (\bar{D}-1)}\right], \tag{34}$$

where,

$$\mu_o = 2 \left[\frac{\eta V_2}{D_2 p} \cdot \frac{\bar{\sigma}_2}{p} \right]^{\frac{1}{2}}.$$ (35)

Using equation (2), this reduces to,

$$\mu_a = \frac{\mu_o}{\sqrt{2}} \sqrt{\frac{f \sin \alpha}{W_1}} \left[\frac{\sqrt{(1-R) \exp(\bar{c})}}{(1-C_1) \sqrt{(1-R) \exp(\bar{c})} + C_1} \right]$$ (36)

2.5.2 Strain Hardening Effect:

During plastic deformation the material strain hardens and the nature of the strain-hardening curve depends on the material. But for **rigid** plastic strain-hardening material, Ludwik's power law [12] can be used to account for the effect of strain-hardening. After neglecting the temperature and strain-rate effects for the time being, the strain-hardening effect is given by,

$$\bar{\sigma} = \bar{\sigma}_o + B(\bar{c})^m,$$ (37a)

where $\bar{\sigma}_o$, B and m are material constants.

Jaoul and his co-workers [10] have suggested that experimental curves can be divided into several regions, each characterised by an equation such as equation (37a). Depending upon the material properties, the strain-hardening effect can be evaluated using various mathematical expressions. One of the most general relationship is given by Mellor [19] as

$$\bar{\sigma} = A' (B' + \bar{c})^{n'},$$ (37b)

where A', B' and m' are material constants.

2.5.3 Redundant Work:

In practice, the deformation in wire drawing is inhomogeneous and hence, the energy required for the deformation is more than the minimum energy required for homogeneous deformation. In the case of inhomogeneous deformation, internal shearing can occur which does not contribute to the observed change of shape as shown by the distortion of internal grids during extrusion and rolling [10] and additional work is required for deformation. To account for this redundant work during the process, $\bar{c}$ in equations (1) and (37a) will be replaced by $\bar{e}^* = f\bar{c}$. Therefore, from equations (1), (36) and (37a),

$$\frac{d\sigma_x}{d\bar{c}} + \frac{\mu_o}{\sqrt{2}}\sqrt{\frac{f \, \text{Sin} \, \alpha}{W_1}} \cdot \text{Cot} \, \alpha \cdot \left[\frac{\sqrt{(1-R) \, \exp{(\bar{c})}}}{(1-C_1)\sqrt{(1-R) \, \exp{(\bar{c})}} + C_1} \right] \sigma_x$$

$$= \bar{\sigma}_o \left[1 + \frac{B}{\bar{\sigma}_o} \bar{c}^n\right]\left[1 + \frac{\mu_o}{\sqrt{2}}\sqrt{\frac{f \, \text{Sin} \, \alpha}{W_1}} \cdot \text{Cot} \, \alpha \cdot \right.$$

$$\left. \frac{\sqrt{(1-R) \, \exp{(\bar{c})}}}{(1-C_1)\sqrt{(1-R) \, \exp{(\bar{c})}} + C_1} \right]. \qquad (38)$$

The end-conditions of this equation are:

at entrance:

$$\sigma_x = t_1 \; ; \; \bar{c}_1 = 0 \; , \qquad (39)$$

and at exit:

$$\sigma_x = t_2 \; ; \; \bar{c}_2 = f \ln\left(\frac{1}{1-R}\right).$$

After defining a new variable $\sigma_x' = \sigma_x/\bar{\sigma}_o$, equations (38) and (39) reduce to

$$\frac{d\sigma_x'}{d\bar{e}} + \frac{\mu_o}{\sqrt{2}}\sqrt{\frac{f\,\mathrm{Sin}\,\alpha}{W_1}}\cdot\mathrm{Cot}\,\alpha\cdot\left[\frac{\sqrt{(1-R)\,\exp(\bar{e})}}{(1-C_1)\sqrt{(1-R)\,\exp(\bar{e})}+C_1}\right]\sigma_x'$$

$$= \left[1+\frac{B}{\sigma_o}\bar{e}^m\right]\left[1+\frac{\mu_o}{\sqrt{2}}\sqrt{\frac{f\,\mathrm{Sin}\,\alpha}{W_1}}\cdot\mathrm{Cot}\,\alpha\right.$$

$$\left.\frac{\sqrt{(1-R)\,\exp(\bar{e})}}{(1-C_1)\sqrt{(1-R)\,\exp(\bar{e})}+C_1}\right], \tag{40}$$

And

$$\sigma_x' = \frac{t_1}{\sigma_o} = T_1 \; ; \quad \bar{e}_1 = 0 \; ,$$

$$\sigma_x' = \frac{t_2}{\sigma_o} = T_2 \; ; \quad \bar{e}_2 = f\,\ln\left(\frac{1}{1-R}\right), \tag{41}$$

where T_1 and T_2 are dimensionless drawing stresses.

2.5.4 Strain-Rate and Temperature Effects:

Because of high speeds involved in wire drawing, strain-rate hardening takes place. At the same time, part of the total energy supplied for deformation is absorbed by the material and raises its temperature. Temperature and strain-rate are related with respect to their effects on the stress-strain curves for metals; an increased strain-rate has similar effect as lowering of temperature, and vice versa [10]. For accounting the effects of strain-rate and temperature at a particular value of strain, a commonly used

relationship is of the form [10],

$$\sigma_e = g(z),$$
(42)

and $z = \dot{\varepsilon} \exp (\Delta H / R'T),$

where ΔH is the activation energy, $\dot{\varepsilon}$ is strain-rate, z is the Zener-Hollomon parameter, R' is the gas constant, T is absolute temperature and σ_e is the stress at a given strain e. Since the interpretation of the activation energies obtained, is by no means straight forward and hence the parameter holds only over narrow ranges of strain-rate and temperature [10]. Further simplification of equation (42) results in

$$\sigma_e = K [\dot{\varepsilon} \exp (\frac{\Delta H}{R'T})]^n,$$
(43)

where n is a function of temperature and reduction,

K is the yield stress at a given strain and is given by

$$K = \bar{\sigma}_0 + B \bar{e}^m.$$
(44)

Therefore, including the effects of strain, strain-rate and temperature, the generalised yield-stress can be evaluated from,

$$\bar{\sigma} = (\bar{\sigma}_0 + B \bar{e}^m) [\dot{\varepsilon} \exp (\frac{\Delta H}{R'T})]^n.$$
(45)

In order to simplify the analysis only an average value of effective strain-rate will be considered.

2.5.4.1 Evaluation of Average Effective Strain-Rate:

The value of strain-rate varies along the axial as well as transverse directions. Therefore, for all practical purposes, Avitzur [2] suggested an average value of the strain-rate and evaluated it from the expression,

$$\bar{\dot{\varepsilon}} = \frac{1}{v} \int_v \dot{\varepsilon} \, dv = \frac{2}{3v} \int_v \sqrt{\frac{1}{2} \dot{\varepsilon}_{ij} \cdot \dot{\varepsilon}_{ij}} \, dv \, , \qquad (46)$$

where ε_{ij} is the strain at plane i in direction j, and

v is the volume of the deformation zone II as shown in Fig.2.2 and can be evaluated from,

$$v = \frac{2\pi}{3} \cdot \frac{1 - \cos \alpha}{\sin^3 \alpha} (R_1^3 - R_2^3) \simeq \frac{2\pi}{3} \cdot \frac{(R_1^3 - R_2^3)}{(1 + \cos \alpha) \sin \alpha} \, ,$$

where, $\qquad\qquad\qquad\qquad\qquad\qquad\qquad\qquad\qquad\qquad (47)$

$$R_1 = D_1/2 \, ,$$

and $\qquad\qquad\qquad\qquad\qquad\qquad\qquad\qquad\qquad\qquad (48)$

$$R_2 = D_2/2 \, .$$

As shown in Fig. 2.2, the deformation zone is bounded by the surface of the die with a cone of included angle 2α and two concentric surfaces L_1 and L_2. Assuming spherical coordinate system (r, θ, ϕ) in the deformation zone, the strain-rates, in the case of axial cylindrical symmetry with respect to ϕ axis, reduce to,

$$\left. \begin{aligned} \dot{\varepsilon}_{rr} &= -2 \, \dot{\varepsilon}_{\theta\theta} = -2 \, \dot{\varepsilon}_{\phi\phi} = 2V_2 \, r_f^2 \, \frac{\cos \theta}{r^3}, \\ \dot{\varepsilon}_{r\theta} &= \frac{1}{2} V_2 \, r_f^2 \, \frac{\sin \theta}{r^3}, \\ \dot{\varepsilon}_{\theta\phi} &= \dot{\varepsilon}_{r\phi} = 0 \, . \end{aligned} \right\} \quad (49)$$

where r_f is the radius of concentric surface L_2.

Substituting these values of the strain-rates in equation (46) and integrating, we get

$$\bar{\dot{\varepsilon}} = \frac{2\dot{v}}{v} . F(\alpha). \ln \left(\frac{R_1}{R_2}\right), \tag{50}$$

where $\dot{v}$, the volume flow-rate of the deformed material is given by,

$$\dot{v} = \pi V_2 R_2^2, \tag{51}$$

and

$$F(\alpha) = \frac{1}{\sin^2 \alpha} \left[1 - \cos \alpha \sqrt{1 - \frac{11}{12} \sin^2 \alpha} \right.$$

$$\left. + \frac{1}{\sqrt{(11 \times 12)}} \ln \left[\frac{1 + \sqrt{\frac{11}{12}}}{\sqrt{\frac{11}{12}} \cos \alpha + \sqrt{1 - \frac{11}{12} \sin^2 \alpha}} \right] \right]. \tag{52}$$

Hence from equations (47), (50) and (51), the average effective strain-rate is given by,

$$\bar{\dot{\varepsilon}} = \frac{3}{2} \frac{V_2}{R_2} \frac{(1 + \cos \alpha) \sin \alpha . F(\alpha)}{(R_1/R_2)^3 - 1} . 2 \ln (R_1/R_2). \tag{53}$$

This value of the average effective strain-rate can be used in equation (45) to evaluate the generalised yield stress.

2.5.4.2 Temperature Dependence of n:

In equation (43), the value of n depends on temperature as well as reduction. Alder and Phillips [11] have pointed out that the value of strain-rate index (n) depends on the

homologous temperature (T_H) and the amount of compression.
Assuming wire drawing as a closed compression problem [8],
the effect of temperature and reduction can be incorporated
in evaluating n. However, an empirical relationship can be
obtained for evaluating n. This has been obtained from the
experimental data of Alder and Phillips [11] and gives this
relationship as,

$$\frac{n}{T_H} = .04 + 5 \times 10^{-4} R .$$ (54)

Equation (54) holds only for the range of temperatures less
than $0.55 T_m$, where T_m is the melting point temperature of
the material. For higher values of temperature, the slope
of the curve changes and equation (54) is not valid. In wire
drawing operations, the temperature rise is generally small
since most of the heat generated is carried away by the
lubricant. Experiments indicate that only about 10 percent
of the heat generated is absorbed into the work-material [10].
Using equations (45), (53) and (54) the generalised yield
stress is,

$$\bar{\sigma} = [\bar{\sigma}_0 + B \bar{c}^m][\bar{\varepsilon} \exp (\frac{\Delta H}{R'T})]^n ,$$ (55)

where,

$$\bar{\varepsilon} = \frac{3}{2} \frac{V_2}{R_2} \frac{(1+\cos \alpha) \sin \alpha \; F(\alpha)}{(R_1/R_2)^3 - 1} . 2 \ln (R_1/R_2),$$

and

$$n = (.04 + 5 \times 10^{-4} R) T_H .$$

The stress distribution can now be evaluated by substituting equation (60) in equation (1).

Thus the effects of strain, strain-rate, temperature, lubrication, reduction etc. can be incorporated in the analysis of the wire drawing operation. For a strain-hardening material the variation of drawing stress with semi-die angle and reduction as parameter can be evaluated using equations (11), (27), (30.), (40) and (41). For incorporating the effects of strain-rate along with strain-hardening, the activation energy (ΔH) in equation (55) is taken as zero and $T_H = 1$ is substituted in equation (54). Now, using equations (1), (36), (54) and (55) we can calculate the variation of **drawing** stress with semi-die angle, taking reduction as a parameter. And to incorporate all the effects considered, use of equations (1), (53), (54) and (55) are made. After introducing the effects of various parameters, a differential equation of the following form is obtained,

$$\frac{dy}{dx} = f(x, y, \alpha, R, V, T),$$

where

$$y(x_1) = y_1 \text{ (unknown)}, \quad y(x_n) = y_n \text{ (unknown)},$$
$$y_1/y_n = \text{Constant (known)}.$$

The fourth order Runge-Kutta method can be used for obtaining numerical solution of this equation.

CHAPTER III

RESULTS AND DISCUSSION

Numerical results have been obtained for the set of input data given in Appendix 1. This data has been taken from reference [15]. Theoretical results have been obtained on computer using equations derived in the previous chapter. Since the published experimental results on wire drawing are very limited, most of the figures give theoretical results. Wherever possible, results have been compared with previously published experimental values.

Minimum film thickness has been theoretically evaluated for the experimental conditions used by Christopherson and Naylor [3]. The strain-hardening curve for the soft copper wire used has been taken from [19], and is given in Appendix 1. It has also been assumed that the surface conditions of wire and die are such that hydrodynamic lubrication is achieved. The minimum film thickness for this condition was calculated to be 1.07×10^{-4} cm. which is of the same order of magnitude as measured by Christopherson and Naylor [3].

For the same drawing conditions, Bedi's analysis [15] gives the minimum film thickness as 1.44×10^{-4} cm. The difference between Bedi's and present result is primarily because of the assumption made regarding the variation of film thickness within the die. While Bedi assumed this film thickness variation to be exponential, in the present work it is assumed to have a linear variation.

Fig. (3.1) shows the variation in lubricant film thickness within the die for various reductions. The film thickness appears to increase as the reduction increases but this variation is not very significant.

Figures (3.2) and (3.3) show the variation of apparent coefficient of friction with semi-die angle at entrance and exit, respectively. For comparison, Bedi's results [15] using exponential variation in film thickness are also shown in these figures. These figures clearly show that the apparent coefficient of friction at both entrance and exit increases with increasing semi-cone angle. Not only the general pattern of the curve but also the magnitude of apparent coefficient of friction is very close to those obtained by Bedi [15].

Fig. (3.4) shows the variation of apparent coefficient of friction with reduction at the exit section of the die.

Again for comparison, Bedi's results are also shown and it
is clear that the nature of the two curves are quite similar.

In Fig. (3.5), the dimensionless drawing stress has been
plotted against semi-die angle for various values of reduc-
tions. It is seen that there is an optimum die angle, at
least in the range of lower reductions. The optimum die
angle, however, appears to vary with reduction. The value
obtained in the present case appears to be around 2 degrees.
The range of values for optimum die-angle obtained by
Wistreich [4], Avitzur [2], and Green [16] was in the range
of 2 to 4 degrees. In these earlier theories, the coefficient
of friction was assumed to be constant, while in the present
work this varies with the semi-cone angle, being zero at
$\alpha = 0$. The curves in Fig.(3.5) also show that there exists
a maxima for optimum die-angle and that there exists no
optimum die-angle at high reductions. This may be because
of the fact that apparent coefficient of friction decreases
rapidly with increase in reduction (Fig. (3.4)) while the
redundant work decreases with increase in reduction. This
does not allow the frictional work to balance the redundant
work and results in no optimum die angle at high reductions.
Again Bedi's results for exponential film thickness are shown
for comparison and shows close agreement. It may be mentioned
that wire drawing can not be carried out at high reductions suc

as 0.6. The curves for higher reductions have been merely shown to indicate the variation in optimum die-angle with reduction.

Comparison of present results with those obtained by Bedi show fairly close agreement. This provides ample justification for using a simpler model of linear film thickness variation within the die. Such an assumption not only simplifies the analysis considerably and reduces computation time but also enables the extension of the theory to incorporate the effects of other parameters such as strain-hardening, strain-rate, temperature etc. without unnecessarily complicating the analysis. Results so far quoted did not include the effects of strain-rate and temperature.

Fig. (3.6) shows the variation of dimensionless drawing stress with semi-cone angle. These results have been obtained after including the effects of strain as well as strain rate hardening. The nature of curves remain same as in previous case (Fig. (3.5)) except that the drawing stress shows a higher value while the optimum die angle is slightly in the lower range. This reduction in optimum die-angle is most probably due to cumulative effect of shear and frictional losses. The shear losses increase with increasing strain rate hardening while the frictional losses remain more or less constant.

Plots of variation of dimensionless drawing stress with semi-die angle at various reductions are shown in Fig. (3.7). It incorporates the effect of strain-hardening and strain-rate and temperature effects. Again the nature of curves are same except for higher values of optimum die-angle. In this case, the softening of the work material due to temperature effects results in decrease in shear work. Again, assuming the friction losses to remain same, a higher value for optimum die-angle would be expected. Hill and Tupper [20] have also shown that for a given reduction, the frictional contribution to the drawing stress decreases as die-angle increases while the contribution from non-useful work increases. The present results seem to indicate this to be the case.

For comparison, the effects of strain, strain-rate and temperature on drawing stress are shown in Fig. (3.8).

When optimum die-angles are plotted against reduction (Fig. (3.9)), an optimum value is again obtained. Based on the results of Weiss [21], Linicus et.al.[22], Hill and Tupper [20] indicate a linear variation of optimum die-angle with reduction for very low and constant value of coefficient of friction. The present result, also indicates that for a strain, strain-rate and temperature sensitive material the optimum die-angle increases linearly but at

high reductions the curve is no longer linear. This is
apparently because of the fact that the apparent coefficient
of friction decreases rapidly with increase in reduction
(Fig. (3.4)), while it increases as semi-die angle increases
(Fig. (3.2) and Fig. (3.3)). As indicated earlier, higher
values of optimum die-angles are obtained when the strain
rate and temperature effects are incorporated. The pattern
of this variation of optimum die-angle with reduction also
agrees qualitatively with the experimental results of
Wistreich [6] who found this variation to be almost linear.

For comparison with published experimental results [6]
the theoretical results have again been obtained for various
values of reduction. The drawing conditions used by
Wistreich [6] are given in Appendix 1. Assuming a temperature
rise of around 100 degrees, (i.e. a homologous temp. = 0.35),
the dimensionless drawing stress was calculated for various
values of semi-die angle. These results are shown in
Fig. (3.10) which indicates reasonably good agreement
between theoretical and experimental results.

CHAPTER IV

CONCLUSION

The theoretical analysis for wire-drawing incorporating the effects of strain, strain-rate, temperature and lubricant appears to yield results which are reasonably close to the published experimental values. The calculated value of minimum film thickness is also close to the measured value. The assumption of linear variation of film thickness within the die also appears to be reasonable since it yields results which agree qualitatively with the experimental **values** . This approximation simplifies the analysis considerably and allows for introduction of strain, strain-rate and temperature effects without making the analysis cumbersome.

Results indicate that the apparent coefficient of friction increases with increase in semi-die angle but decreases with increase in reduction. Their also exists an optimum die-angle which gives minimum drawing stress. This optimum value, however, depends on reduction. For strain, strain-rate and temperature sensitive materials, the optimum die-angle increases linearly in the practical range of reductions.

REFERENCES

1. Rabinowicz,E., 'Friction and Wear of Materials', John Wiley and Sons, New York, 1965.

2. Avitzur, B., 'Metal Forming: Processes and Analysis', McGraw Hill, New York, 1968.

3. Christopherson,D.G. and Naylor, H., 'Promotion of fluid Lubrication in Wire Drawing', Proc. Inst. Mech.Engrs. Vol. 169, pp. 643, 1955.

4. Wistreich, J.G., 'The Fundamentals of Wire Drawing', Metall.Rev.Vol.3, pp. 97, 1958.

5. Bland, D.R. and Ford, H., 'Cold Rolling with Strip Tension Part III - An Approximate Treatment of the Elastic Compression of the Strip in Cold Rolling', J. Iron and Steel, Vol. 171, pp. 245, 1952.

6. Wistreich, J.G., 'Investigation of the Mechanics of Wire Drawing', Proc. Inst. Mech.Engrs., Vol.169, pp. 659, 1955.

7. Yang, C.T., 'On the Mechanics of Wire Drawing', Trans. A.S.M.E. Ser.B, Vol. 83, pp. 523, 1961.

8. Crook, A.W., 'The Lubrication of Rollers', Phil.Trans. Roy.Soc., Vol. A 250, pp. 387, 1958.

9. Shaw, M.C.,and Macks, F ., 'Analysis and Lubrication of Bearings', McGraw Hill, New York, 1949.

10. Tegart, W.J.M., 'Elements of Mechanical Metallurgy', Macmillan, New York, 1966.

11. Alder, J.F. and Phillips, V.A., 'The Effect of Strain-Rate and Temperature on the Resistance of Aluminium , Copper and Steel to Compression', J.of the Inst. of Metals, Vol. 83, No.3, pp. 80, 1954/55.

12. Johnson, W. and Mellor, P.B., 'Plasticity for Mechanical Engineers', Von Nostrand, London, 1962.

13. Lal,G.K., and Hillier, M.J., 'The Expansion of a Thin Free Tube in Electro Magnetic Forming', Int. J. Prod. Res., Vol. 8, No.1, pp. 59, 1970.

14. Hillier,M.J., 'A Hydrodynamic Model of Hydrostatic Extrusion,' Int.J.Prod.Res. Vol.5, pp. 171,1967.

15. Bedi,D.S., 'A Hydrodynamic Model for Wire Drawing', Int.J.Prod.Res., Vol.6, pp. 329, 1968.

16. Green,A.P., 'Plane Strain Theories of Drawing', Proc. Inst. Mech. Engrs., Vol. 174, pp.847,1960.

17. Pinkus,O. and Sternlicht, B., 'Theory of Hydro-dynamic Lubrication', McGraw Hill, New York, 1961.

18. Rowe, G.W., 'An Introduction to the Principles of Metal Working', London: Arnold, 1965.

19. Mellor, P.B., 'The Ultimate Strength of thin Walled Shells and Circular Diaphrams Subjected to Hydrostatic Pressure', Int.J.Mech.Sci., Vol. 1, pp.216,1960.

20. Hill, R. and Tupper, S.J., 'A New Theory of Plastic Deformation in Wire Drawing', J. Iron Steel Inst., Vol. 159, pp. 353, 1948.

21. Weiss,L., 'Zeitschrift fur Metalkunde', Vol. 19, pp. 161, 1927.

22. Linicus,W. and Sachs,'Mitteilungen der deutschen Material prüfungansanstalten', Vol. 16,pp.38,1931.

23. Tattersall,G.H., 'Theory of Hydrodynamic Lubrication in Wire Drawing', Brit.Iron Steel Res.Assn.Rept. MW/D/46/59.

24. Lubhahn, J.D. and Felgar,R.P., 'Plasticity and Creep of Metals', Wiley, New York, 1961.
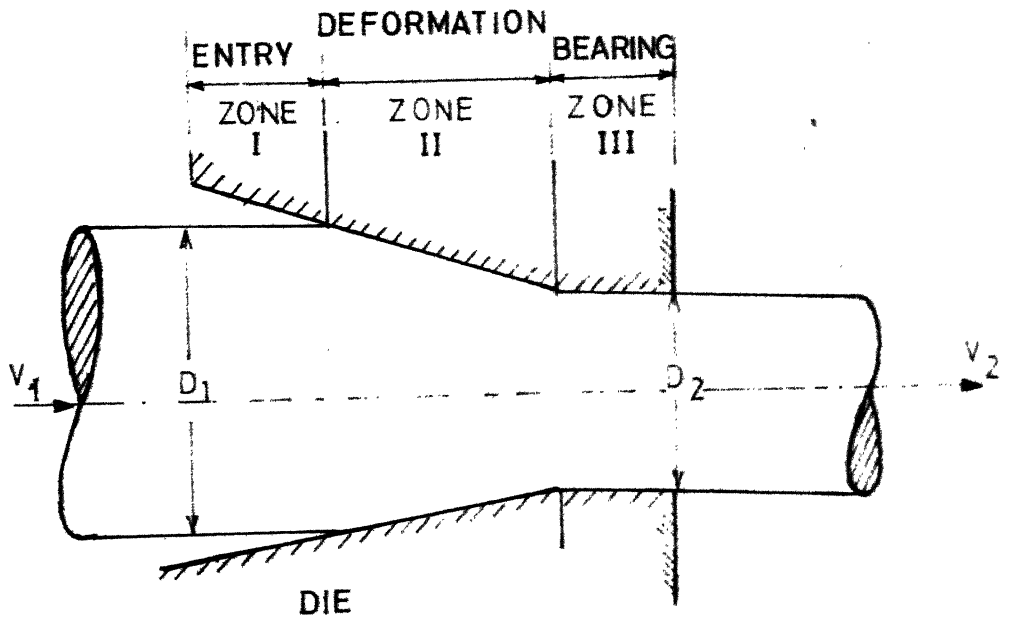
FIG·1·1   WIRE   DRAWING   OPERATION
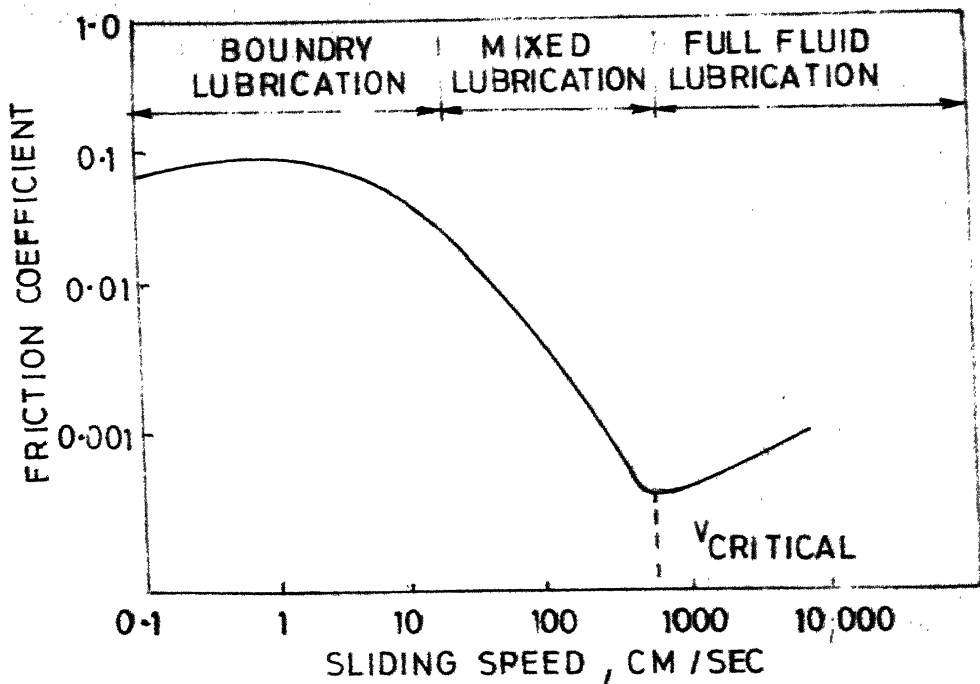
FIG. 1·2   FRICTION-VELOCITY CURVE FOR SURFACES
CAPABLE OF HYDRODYNAMIC LUBRICATION
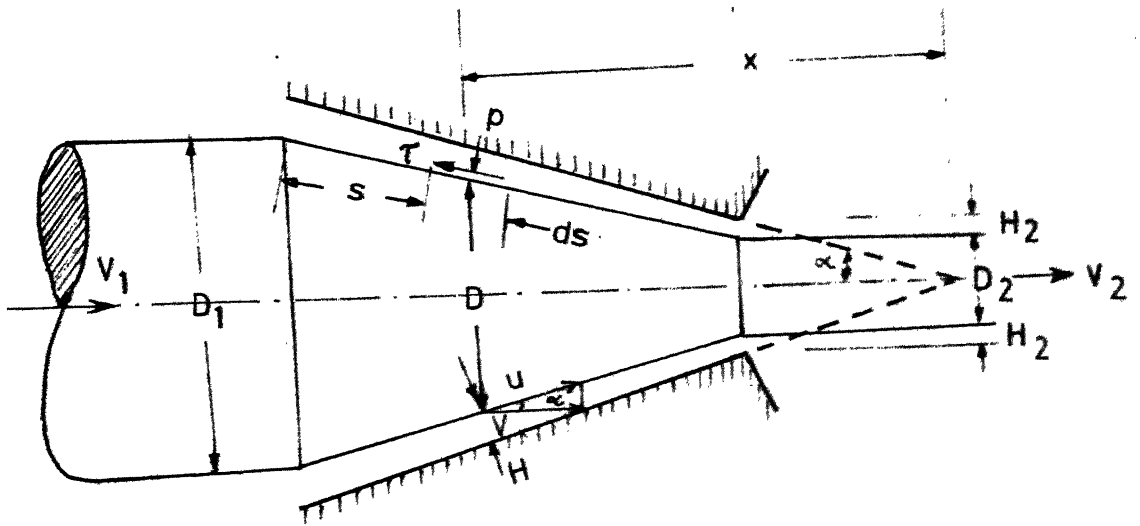
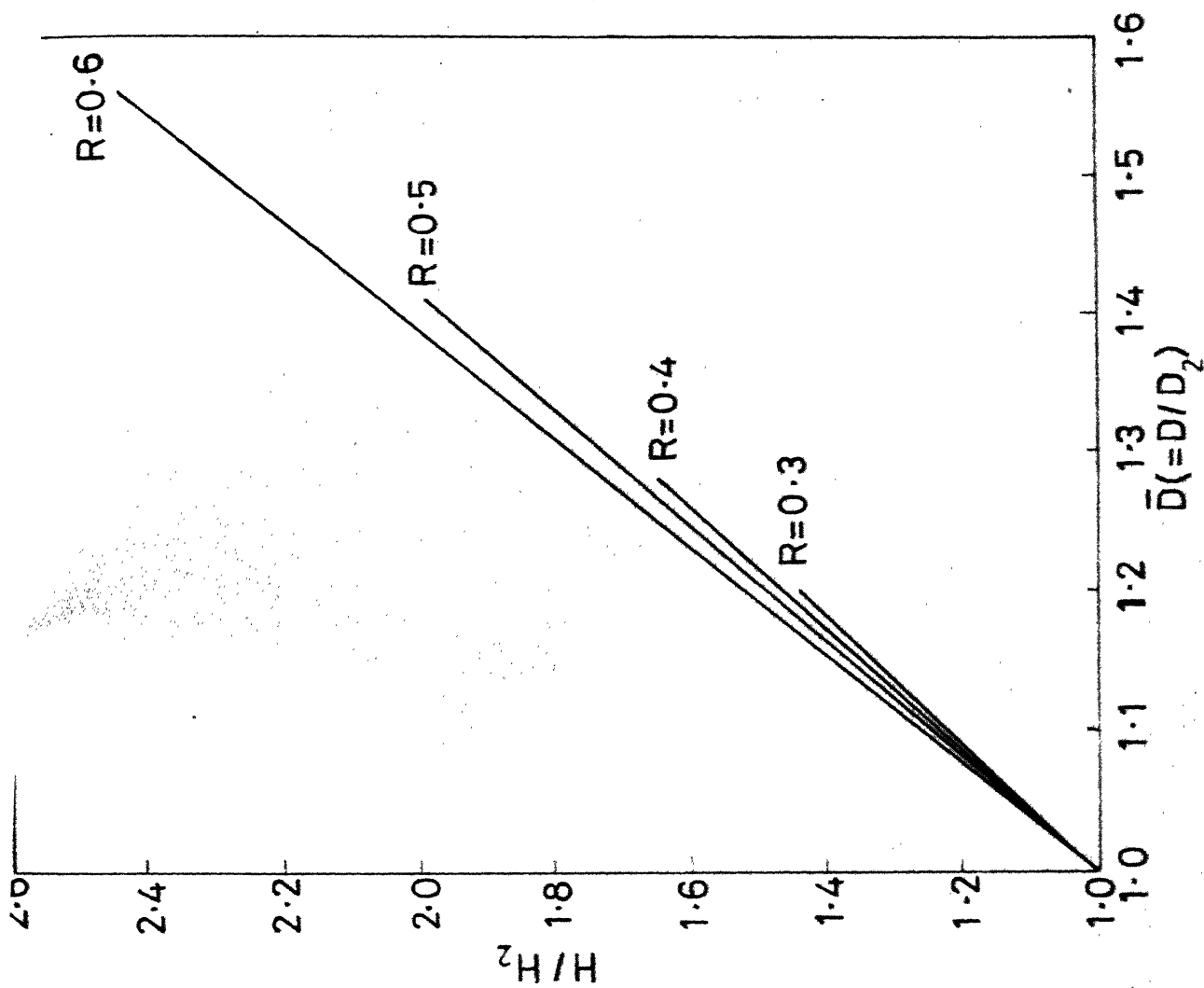FIG. 2·1 STRESSES ON AN ELEMENT OF WIRE MATERIAL
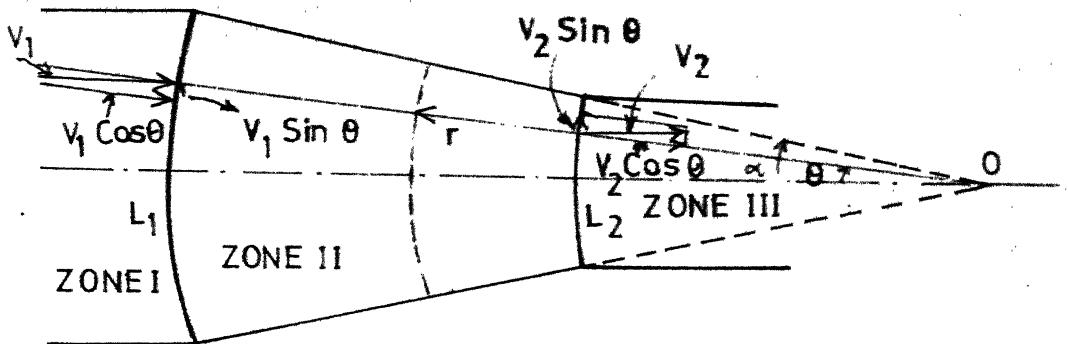
FIG. 2·2 VELOCITY FIELD

FIG.3-1 VARIATION OF DIMENSIONLESS LUBRICATION FILM THICKNESS (H/H_2) WITHIN DIE
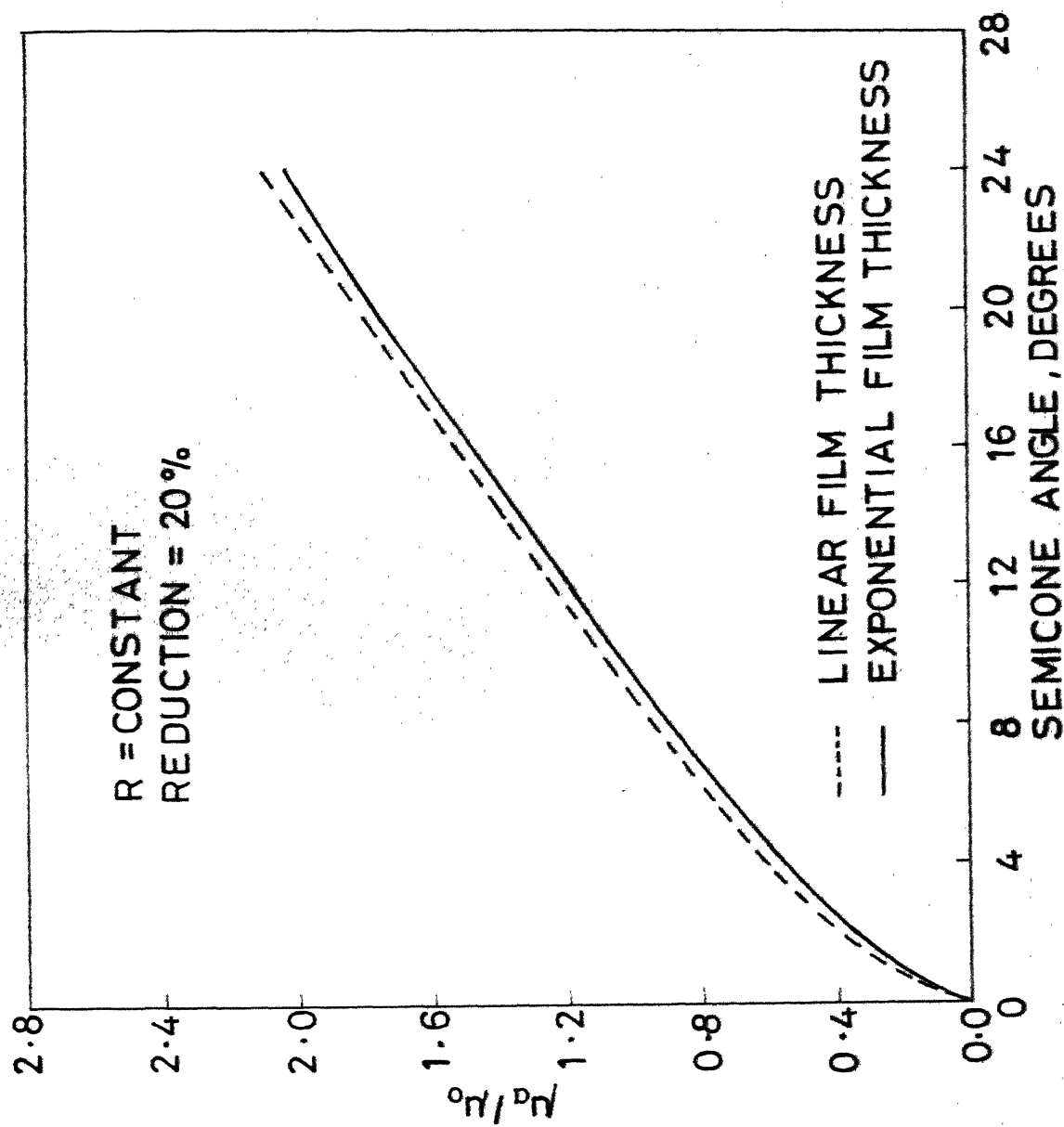
FIG. 3·2 VARIATION OF APPARENT COEFFICIENT OF FRICTION (μ_a/μ_o) WITH SEMICONE ANGLE AT ENTRANCE
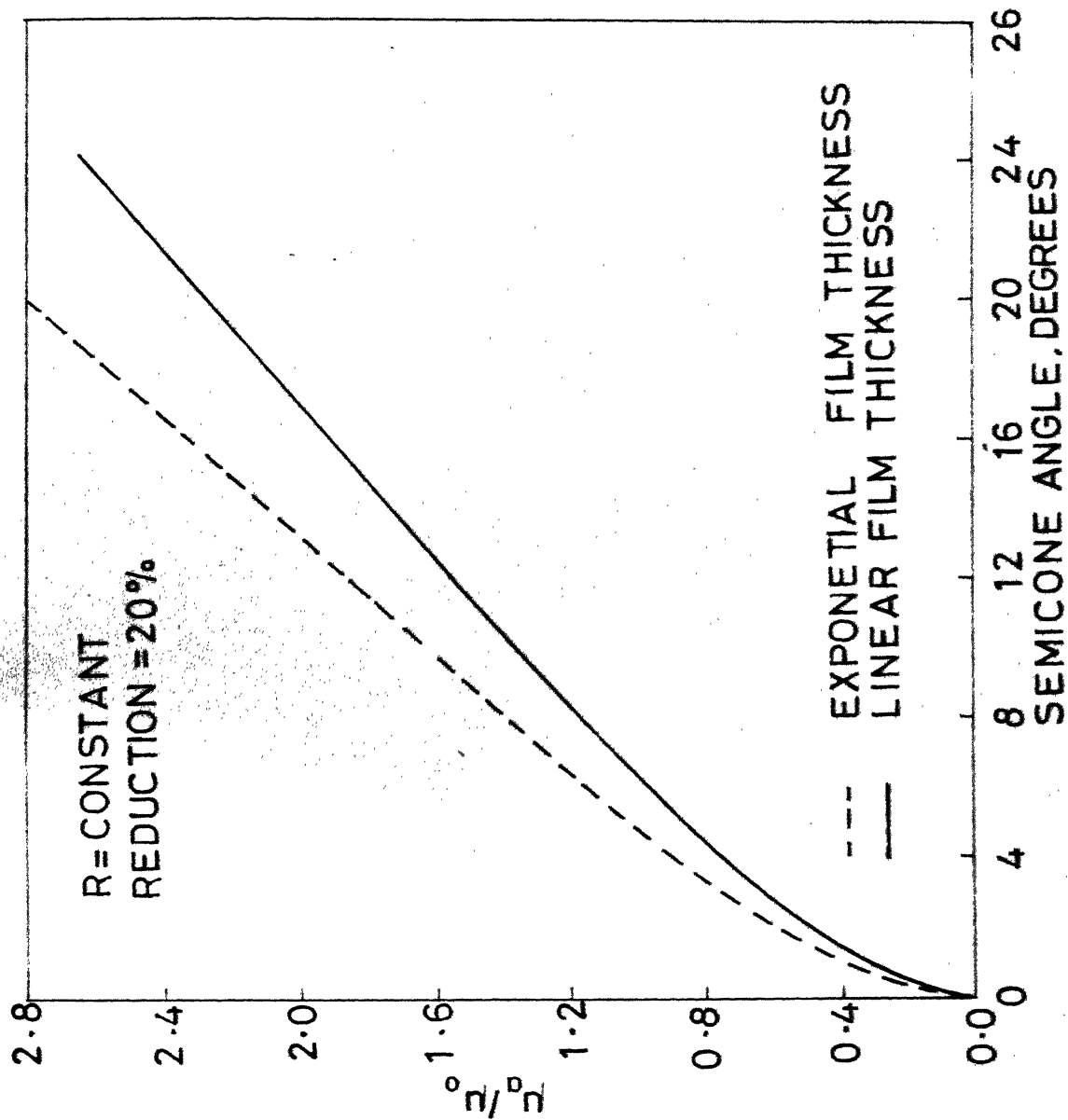
FIG. 3.3 VARIATION OF APPARENT FRICTION COEFFICIENT (μ_a/μ_o) WITH SEMICONE ANGLE AT EXIT
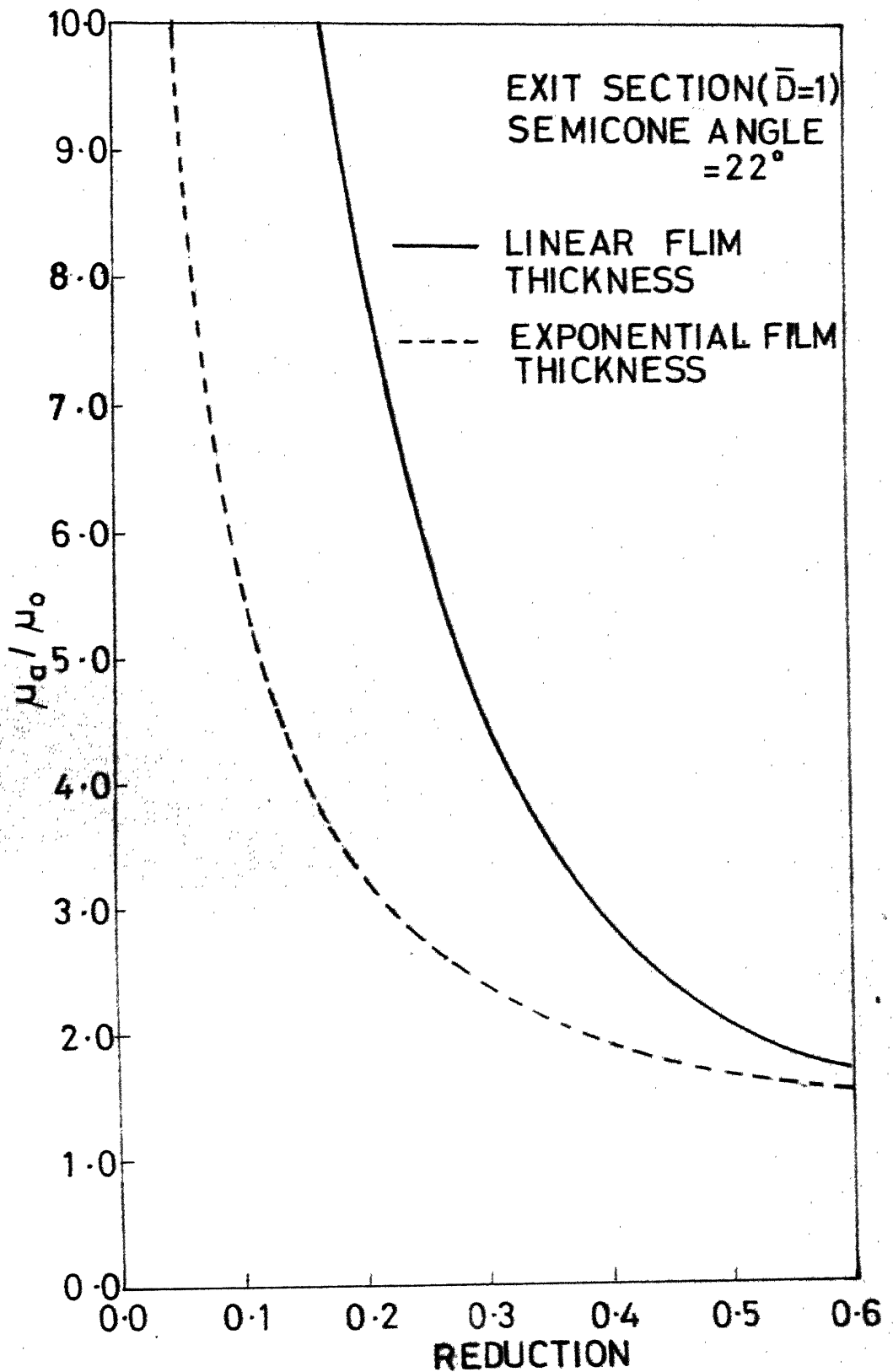
FIG. 3·4 VARIATION OF APPARENT FRICTION COEFFICIEN
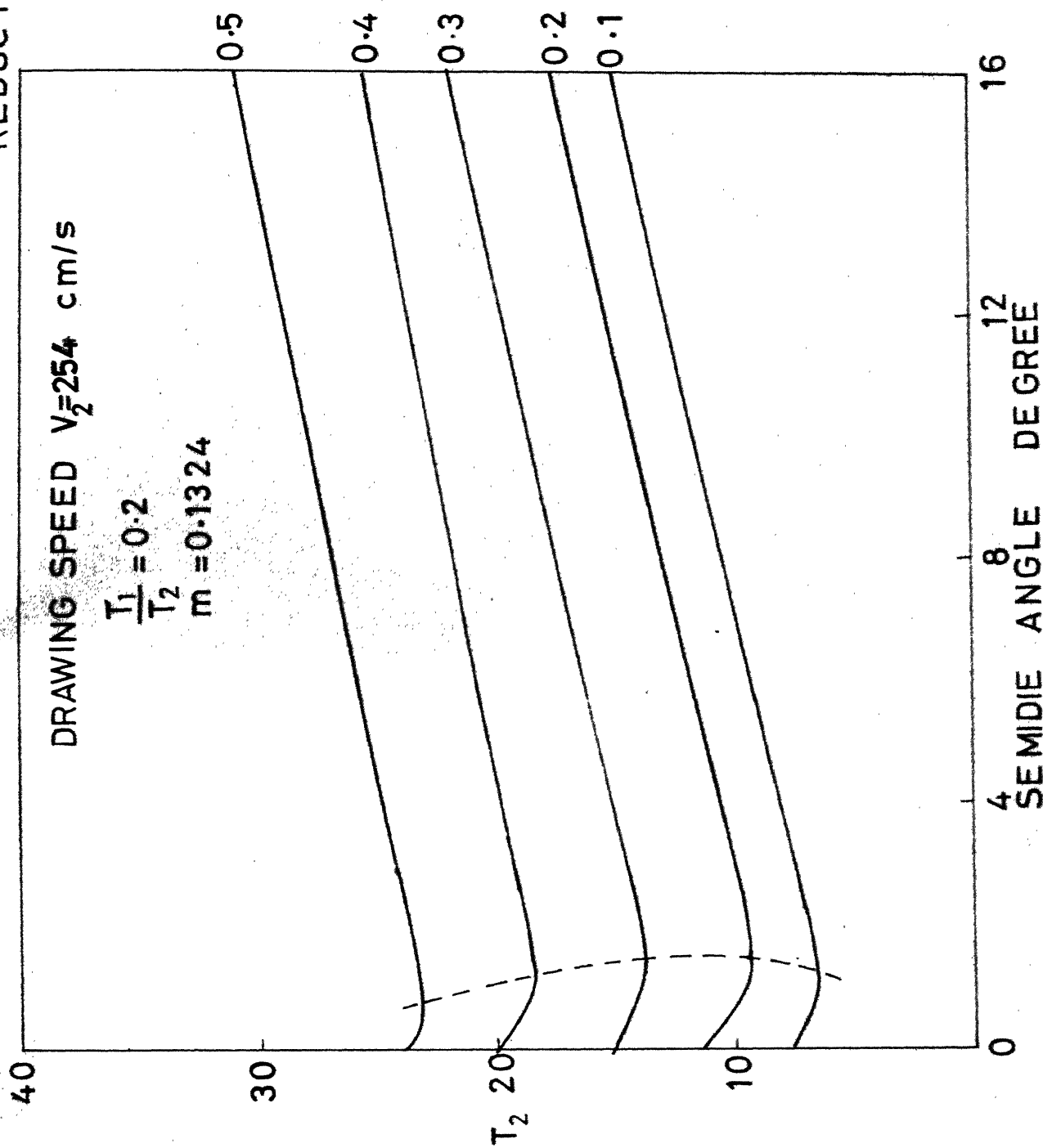(μ_a / μ_o) AT EXIT SECTION WITH   REDUCTION
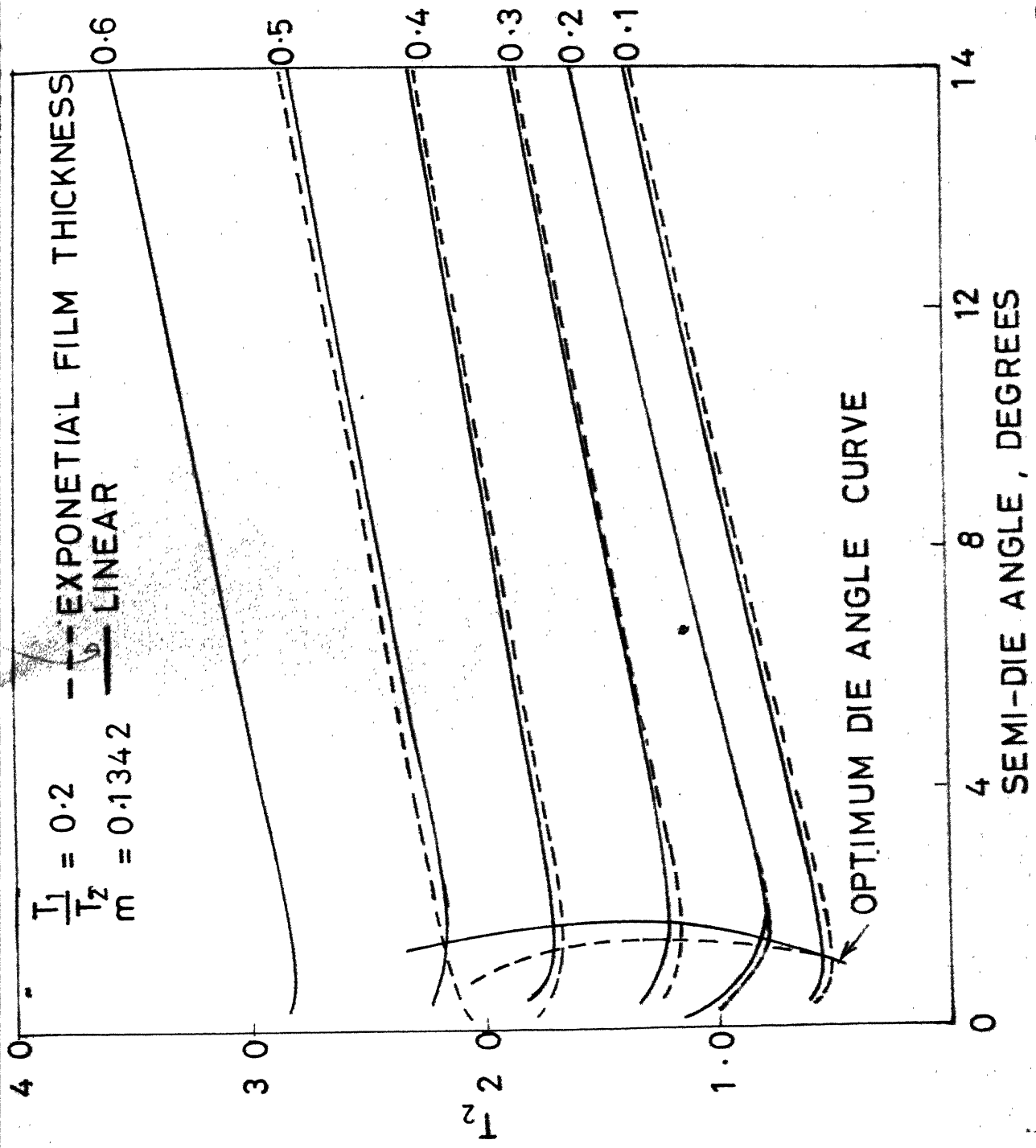
FIG. 3.5 DIMENSIONLESS DRAWING STRESS (T_2) AS FUNCTION OF SEMI-DIE

DRAWING SPEED $V_2 = 254$ cm/s

$\dfrac{T_1}{T_2} = 0.2$

$m = 0.1324$

0.5
0.4
0.3
0.2
0.1

T_2

40

30

20

10

0   4   8   12   16

SEMIDIE ANGLE DEGREE

FIG 3.6   DIMENSIONLESS DRAWING STRESS (T_2) AND REDUCTION AS
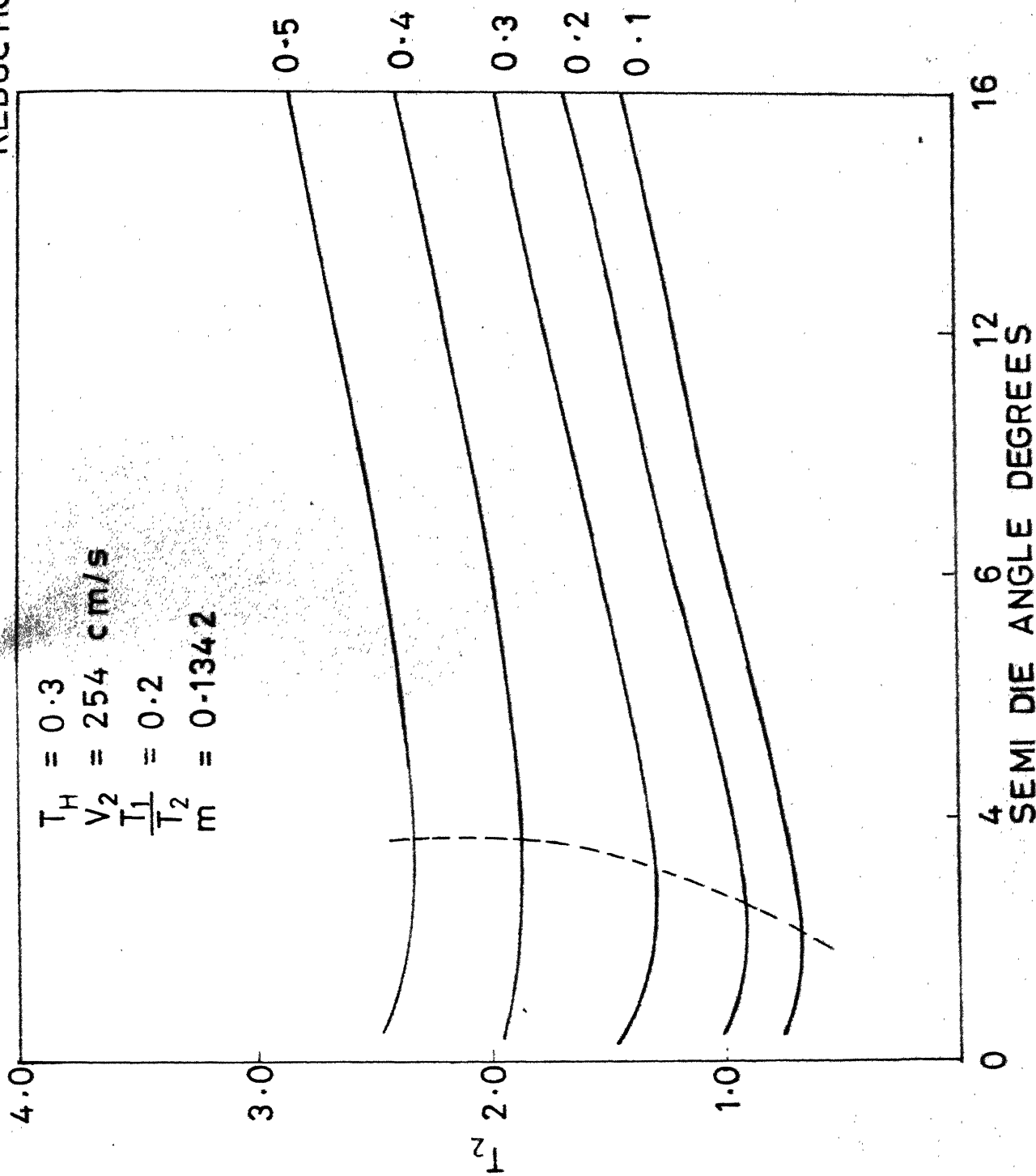
FIG 2.7 DIMENSIONLESS DRAWING STRESS AS FUNCTION OF SEMI-DIE

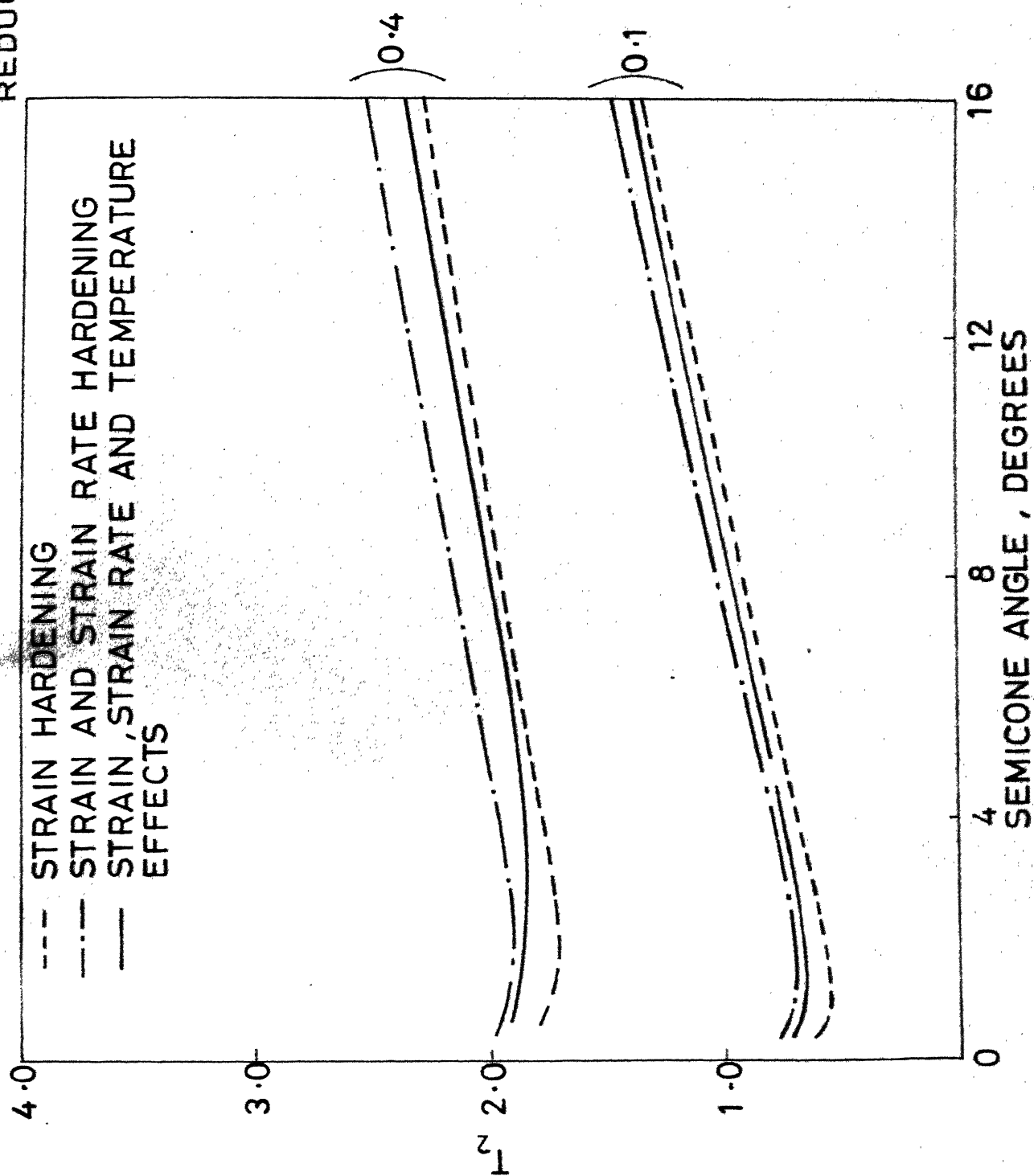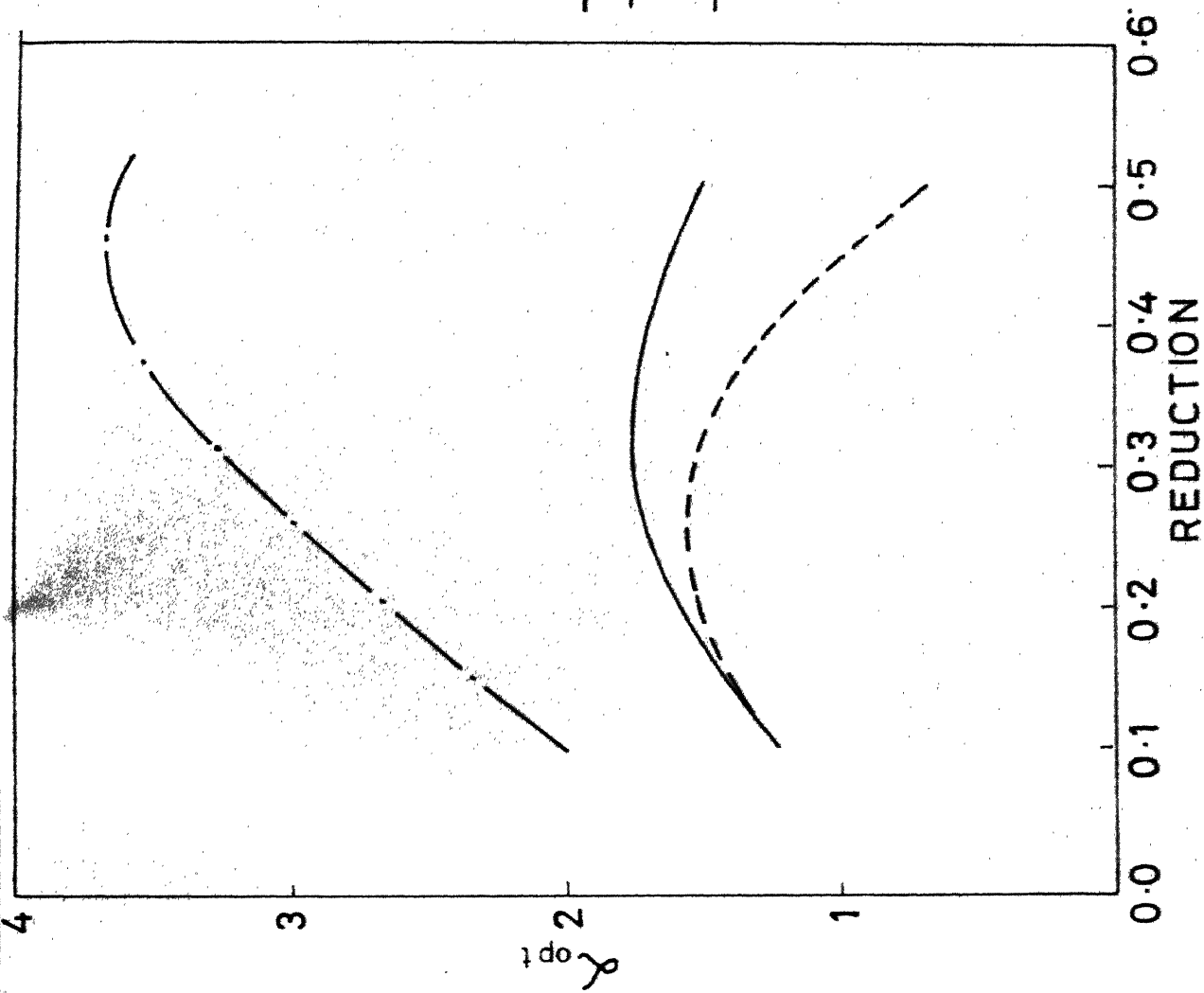FIG. 3.8 COMPARISON OF DIMENSIONLESS DRAWING STRESS AS FUNCTION OF

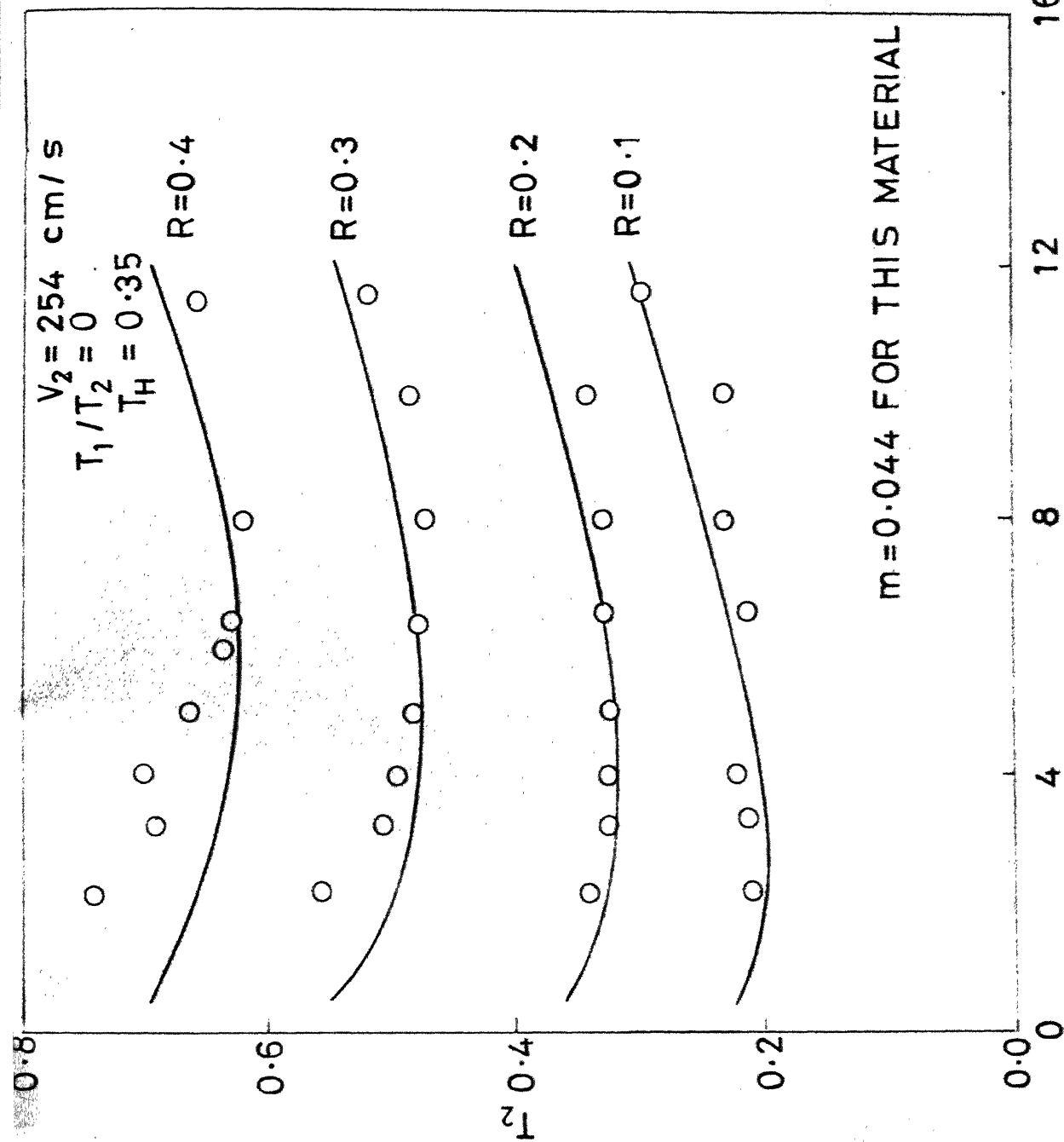FIG. 3.9 VARIATION OF OPTIMUM DIE ANGLE WITH REDUCTION

FIG. 3·10 COMPARISON OF THEORETICAL RESULTS WITH WISTREICH'S

APPENDIX 1

1.1 Minimum Film Thickness:

For evaluating the minimum film thickness H_2, original experimental data of Christopherson and Naylor [3] quoted by Bedi [15] was used. In their experiments a soft copper wire of 0.122 cm diameter was drawn to 0.1067 cm. diameter through a die of 6° included angle. The oil lubricant used had the coefficient of viscosity (η_0) under atmospheric pressure at 25^OC as 3.88 centipoises. The pressure coefficient of viscosity of oil γ as 2.3032 cm^2/Kg. The drawing force was observed as 11.294 Kgf at drawing speed of 304.8 cm/sec. with 4.989 Kgf of estimated tube-drag.

The strain-hardening curve for soft copper is given by Mellor [19] as

$$\bar{\sigma} = 4373.1 \, (.016 + \bar{c})^{0.3}$$

It is assumed that the surface conditions of wire and die were such that at this speed the hydrodynamic conditions were prevailing. The coefficient of viscosity varies exponentially with pressure on the oil film and is given by

$$\eta = \eta_0 \, e^{\gamma \cdot p} \, ,$$

where, η is the viscosity of the oil at pressure p and γ is the coefficient of viscosity. For making the calculation simpler, the average value of the viscosity at average pressure is taken.

1.2 <u>Dimensionless Drawing Stress</u>:

For calculating the variation of dimensionless drawing stress with semi-die-angle, and reduction as parameter, the following data were used. For a wire of low carbon steel (.18 % C) having an initial yield stress of 2812.3 Kg/mm^2, the empirical constants defining the strain hardening curve may be evaluated by Lubhahn and Felgar's [24] method, assuming the non-strain hardening portion of the curve to be of negligible length, to give

$$\bar{\sigma}_0 = 2812.3 \ Kg/mm^2, \quad B = 6468.3 \ Kg/mm^2,$$
$$m = 0.1342$$

1.3 <u>Calculation of Activation Energy</u>:

Stress-strain curves at different temperatures involve two factors: first, the effect of temperature on the flow-stress of a given strain hardened structure; second, the difference in structure produced by a given strain at different temperatures. These effects can be resolved by using a temperature change test in which the metal is strained at a constant strain-rate at some temperature T_{11} to a predetermined strain ε_1, then the temperature is changed suddenly to another temperature T_{22} and new flow-stress is determined by applying a small strain at this temperature. The temperature is then changed rapidly back to T_{11} and the specimen is strained further. This technique enables the reversible change in

flow-stress between two fixed temperatures at a constant strain-rate to be evaluated as a function of strain. Furthermore, the value of $\triangle H$ can be obtained by [10],

$$\triangle H = \frac{R'}{n} \, . \, \ln \left(\frac{\sigma_1}{\sigma_2}\right) . \left(\frac{T_{11} T_{22}}{T_{22} - T_{11}} \right)$$

From the given data [10], $\sigma_1 = 25$ Kg/mm^2 at $T_{11} = 273^{\circ}$K and $\sigma_2 = 49$ Kg/mm^2 at $T_{22} = 180^{\circ}$K, the value of $\triangle H$ can be evaluated.

1.4 Coefficient of friction

To compare with the results of Bedi [15] the coefficient of friction μ_o is taken as 0.025, although, it depends on generalised yield-stress, pressure, viscosity and velocity of the lubricant. But the apparent coefficient of viscosity varies with semi-die-angle and reduction.